S

Caliphate Journal of Science & Technology (CaJoST)

ISSN: 2705-313X (PRINT); 2705-3121 (ONLINE) Research Article

Open Access Journal available at: https://cajost.com.ng/index.php/files and https://www.ajol.info/index.php/cajost/index

DOI: https://dx.doi.org/10.4314/cajost.v8i1.8

Article Info

Received: 23rd January 2026

Revised: 26th February 2026

Accepted: 14th March 2026

Valorisation of *Eleusine indica* Biomass into Functional Carbon Nanomaterials for Controlled Nutrient Delivery and Agronomic Evaluation

Mansur Y. Ibrahim*, Aminu M. Hassan and Hadi Sulaiman

Department of Pure and Industrial Chemistry, Sokoto State University, Sokoto, Nigeria

***Corresponding author's email:**

ymansur64@gmail.com

Cite this: *CaJoST*, 2026, 1, 63-74

This study addresses the environmental drawbacks of intensive synthetic fertilizer use by developing an alternative nutrient-delivery system based on functional carbon nanomaterials (FCNs). The researchers utilized *Eleusine indica* (goose grass), an abundant invasive weed, as a low-cost biomass precursor. The material was converted into FCNs through low-temperature carbonization followed by a modified Hummers-type oxidation process, producing oxygen-functionalized nanoscale carbon structures. Characterization techniques confirmed the successful formation of these nanomaterials. UV–Vis spectroscopy indicated nanosized sp^2 carbon domains, while FTIR and XRD analyses revealed abundant oxygen-containing functional groups and a defect-rich carbon structure. SEM imaging showed crumpled nanosheets with high surface area, suitable for adsorption-based nutrient delivery. The FCNs were used as carriers for NPK fertilizer and tested in a randomized complete block field experiment against controls, organic manure, and conventional fertilizers. Plant growth parameters, including height, leaf number, and leaf width, were monitored over five weeks, alongside elemental uptake analysis. Results demonstrated that FCN-treated plants exhibited slower initial growth but achieved comparable vegetative performance to synthetic fertilizers by the fifth week, indicating sustained nutrient release. Enhanced nutrient uptake further supported their effectiveness. Overall, the study demonstrates that *E. indica* can be valorized into efficient controlled-release nutrient carriers, offering a sustainable approach to improving nutrient-use efficiency while reducing environmental impacts associated with conventional fertilizers.

Keywords: Carbon nanomaterials; carbon dots; invasive weed; nanofertilizer carrier; *Eleusine indica*.

1. Introduction

The pursuit of sustainable agricultural intensification has accelerated interest in nanotechnology-based approaches for improving nutrient delivery efficiency. Conventional bulk fertilizers are often associated with significant environmental losses through volatilisation, leaching, and runoff, whereas nanofertilisers enhance nutrient use efficiency by regulating nutrient availability rather than simply supplying nutrients. Carbon-based nanomaterials have emerged as promising components within this framework, functioning as nutrient carriers, sorbents, or controlled-release agents. Their performance is strongly influenced by physicochemical properties such as surface chemistry, particle size, and interactions within soil–plant systems (Pandey et al., 2024).

Simultaneously, attention has shifted toward the valorisation of underutilised biomass resources into high-value carbonaceous materials. Agricultural residues and invasive weeds offer abundant lignocellulosic feedstocks suitable for thermochemical conversion. Eleusine indica (Paragis or goose grass), a widespread weed with limited economic value, has gained interest due to its high cellulose content (29–61% of dry matter). This makes it a viable precursor for biochar and carbon-based nanomaterial synthesis. Utilizing such biomass supports circular bioeconomy principles by transforming waste into valuable products (Tiba et al., 2025).

Despite these advances, accurate characterisation of biomass-derived nanomaterials remains critical. Terms like "green graphene synthesis" are often used without sufficient evidence, as materials produced via pyrolysis or hydrothermal processes typically resemble carbon dots or graphene-like fragments rather than true graphene. Misclassification can hinder reproducibility and

obscure structure–function relationships. Advances in synthesis highlight the importance of surface functionalisation and heteroatom doping in tailoring material properties (Zamora-Ledezma et al., 2025).

Additionally, the agricultural application of nanofertilisers requires careful assessment of both benefits and risks. While they can improve nutrient delivery, some formulations exhibit phytotoxic effects at high concentrations, affecting plant growth and germination. This underscores the need for standardised evaluation frameworks that integrate agronomic performance with environmental safety (Wang et al., 2025 and Gamal et al., 2025).

This study focuses on evaluating Eleusine indica-derived carbon nanomaterials, aiming to clarify their structure–property relationships and potential role in sustainable nutrient delivery systems.

2. Materials and Methods

2.1 Biomass Collection and Pre-Treatment

Fresh *Eleusine indica* (goose grass) biomass was collected from uncultivated land within Sokoto State University, Nigeria. The biomass was washed sequentially with tap water and distilled water to remove adhering soil and debris. Samples were shade-dried at ambient temperature (27 ± 2 °C) for 7 days until constant mass was achieved. Dried biomass was mechanically milled using a stainless-steel laboratory grinder and passed through a 250 µm mesh sieve to obtain uniform powder (Wang, et al., 2021).

2.2 Carbonization

Carbonization was conducted to obtain a biochar precursor suitable for nanoscale oxidation. The pyrolysis process was conducted using 200 g of biomass on a dry weight basis. The experiment was carried out in a muffle furnace equipped with a nitrogen gas inlet to maintain an inert atmosphere. High-purity nitrogen (99.99%) was supplied at a constant flow rate of 150 mL min^{-1} throughout the procedure. The biomass was heated from ambient temperature to a final temperature of 300 °C at a controlled heating rate of 10 °C min^{-1}. Upon reaching the target temperature, the system was held isothermally for 30 minutes to ensure complete pyrolysis under the specified conditions.

After carbonization, the furnace was allowed to cool naturally to room temperature under nitrogen flow. The resulting biochar was collected and stored in airtight containers for subsequent processing (Chen et al., 2022).

2.3 Particle Size Reduction and Nanoscale Fractionation

Carbonized material was ground using an agate mortar and pestle for 20 min. To isolate nanoscale fractions, 10 g of powdered biochar was dispersed in 500 mL deionized water and ultrasonicated (40 kHz, 300 W) for 45 min. The suspension was allowed to settle for 24 h, after which the supernatant was passed through a 200 nm polycarbonate membrane filter. The filtrate containing nanoscale carbon particles was collected for chemical oxidation.

2.4 Oxidative Functionalization of Carbon Nanomaterials

Functionalized carbon nanomaterials were synthesized using a controlled, modified Hummers-type oxidation method, which is explicitly a chemical oxidation process and not a green synthesis approach. The procedure began by dispersing an amount equivalent to 5.0 g of dry carbon nanomaterials in 250 mL of deionized water under continuous magnetic stirring at 600 rpm. Subsequently, 5.0 g of potassium hydroxide (KOH) was slowly added, and the mixture was stirred for 15 minutes at room temperature. Following this, 15.0 g of potassium permanganate ($KMnO_4$) was introduced gradually over a 30-minute period, with continuous stirring and careful monitoring to ensure the temperature remained below 35 °C. The reaction was then allowed to proceed for 2 hours at 40 °C. To halt the oxidation process, the reaction was quenched by the addition of another 250 mL of deionized water. Finally, the resulting suspension was centrifuged at 5000 rpm for 15 minutes and underwent repeated washing with deionized water until a neutral pH in the range of 6.8 to 7.2 was achieved. The final product was oven-dried at 60 °C for 24 h and stored in desiccators prior to characterization. (Tan et al., 2022).

2.5 Nanomaterial Characterization

The synthesized nanomaterials were characterized using multiple analytical techniques to assess their optical, structural, and morphological properties. UV–Vis spectroscopy was performed across a wavelength range of 200–800 nm using an aqueous dispersion of the sample at a concentration of 0.1 mg mL^{-1}. Fourier transform infrared (FTIR) spectroscopy was conducted over the range of 400–4000 cm^{-1} employing the KBr pellet method to identify functional groups. The crystalline structure was analyzed by X-ray diffraction (XRD) using Cu Kα radiation (λ = 1.5406 Å), with diffraction patterns recorded over a 2θ range of 5–60°. Surface morphology was examined via scanning electron microscopy (SEM) on gold-coated samples at an accelerating voltage of 15 kV (Yahaya et al.,2024).

2.6 Nanofertilizer Formulation

In this study, the functionalized carbon nanomaterials (FCNs) served exclusively as carriers for nutrients rather than as nutrient sources themselves. The formulation was prepared by combining 1.0 gram of FCNs with 10.0 grams of NPK fertilizer (15-15-15) in 200 milliliters of deionized water.

The mixture was stirred for 12 h to allow nutrient adsorption, filtered, and air-dried. This formulation was applied at rates equivalent to recommended NPK application on an equal-nutrient basis (Li et al., 2023).

2.7 Field Experiment Design

The study was laid out in a Randomized Complete Block Design (RCBD) with three replications to evaluate the effects of different fertilizer treatments on the growth of a local leafy vegetable cultivar over a five-week period (Figure `). The four treatments consisted of a control with no fertilizer, organic manure, synthetic NPK fertilizer, and an FCN-based nanofertilizer. To ensure consistency, all fertilizer treatments were applied at nutrient-equivalent rates. Each treatment was assigned to plots measuring 2 meters by 2 meters within each of the three blocks (Chen, et al.,2022).

Figure 1: Demonstration Field Trials Farm for Evaluating the Agronomic Performance of the *Eleusine indica* based Functional Carbon Nanofertilizer compare to artificial fertilizer, compost manure and Control soil

2.8 Statistical Analysis

All agronomic data (plant height, number of leaves, leaf width) were analyzed using analysis of variance (ANOVA) appropriate for a randomized complete block design. The statistical model used was:

$$Y_{ij} = \mu + T_i + B_j + \varepsilon_{ij}$$

Where:

Y_{ij} = observed response

μ = overall mean

T_i = effect of the *i*th treatment

B_j = effect of the *j*th block

ε_{ij} = experimental error

Data were tested for normality and homogeneity of variance prior to analysis. Treatment means were compared using Fisher's Least Significant Difference (LSD) at $p \leq 0.05$. Results are reported as mean ± standard deviation (SD) with sample size (n = 3).-

Statistical analyses were performed using SPSS (version 26.0). Claims of significance were supported by F-values, degrees of freedom, and p-values, and treatment groupings were indicated using letter notation.

2.9 Atomic Absorption Spectroscopy (AAS) Analysis

Elemental concentrations of essential plant nutrients (Ca, Mg, Fe, Zn, and Mn) were determined using atomic absorption spectroscopy (AAS) following wet acid digestion.

2.9.1 Sample Digestion

Oven-dried plant samples were ground to fine powder. A mass of 0.50 g of each sample was accurately weighed into digestion flasks. 10 mL of concentrated nitric acid (HNO_3, 65%) was added to each flask, and the mixture was allowed to pre-digest overnight at room temperature. Digestion was completed by heating the samples on a hot plate at 120 °C for 2 h until clear solutions were obtained. After cooling, digests were filtered and diluted to 50 mL with deionized water.

2.9.2 AAS Instrumentation and Operating Conditions

Elemental analysis was performed using a flame atomic absorption spectrophotometer equipped with element-specific hollow cathode lamps. Instrument calibration was carried out using five-point external calibration curves prepared from certified standard solutions (0, 1, 2, 5, and 10 mg L^{-1}). Each sample digest was analyzed in triplicate instrumental readings, and the mean absorbance value was used for concentration determination.

2.9.3 Quality Control and Data Reporting

Analytical quality was assured through procedural blanks and calibration verification standards analyzed every ten samples. Relative standard

deviation (RSD) of instrumental replicate readings was maintained below **5%**, confirming acceptable instrumental precision. Final elemental concentrations are reported as mean ± standard deviation (SD) of three independent sample replicates (n = 3) and expressed in mg kg^{-1} dry weight.

2.9.4 Detection Limits

Method detection limits (MDLs) were calculated as three times the standard deviation of ten blank measurements and were as follows: Ca (0.02 mg L^{-1}), Mg (0.01 mg L^{-1}), Fe (0.03 mg L^{-1}), Zn (0.01 mg L^{-1}), and Mn (0.02 mg L^{-1}(Nguyen, et al.,2024).

3. Results and Discussion

3.1 Material Identity Clarification

3.1.1 UV-Vis Absorption Spectroscopy Analysis

The interpretation of UV-Vis absorption spectra is fundamental to distinguishing between different carbon-based nanomaterials, particularly graphene oxide (GO), reduced graphene oxide (rGO), and smaller carbonaceous structures like carbon dots. The specific optical behavior observed strong absorption at ~200 nm with notable peak broadening and the absence of a red-shift provides critical structural insights that justify the reclassification of the synthesized material as functionalized carbon nanomaterials (FCNs) as displayed in figure 2.

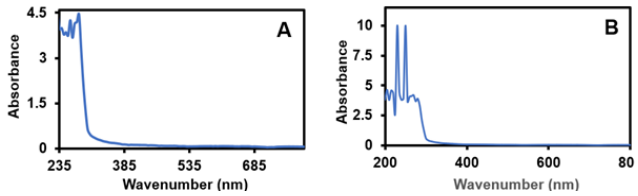

Figure 2: UV-Vis Analysis Results Comparing Free Goose Grass as Control (A) and Goose Grass Synthesised Graphene (B)

The characteristic UV–Vis spectrum of graphene oxide (GO) typically shows a primary absorption peak around 230 nm, associated with π→π* transitions of aromatic C=C bonds, and a shoulder near 300 nm due to n→π* transitions of carbonyl C=O bonds. Upon reduction to reduced graphene oxide (rGO), this main peak generally red-shifts to approximately 260–270 nm, indicating restoration of π-conjugation and increased sp^2 hybridization following the removal of oxygen functional groups (Gomaa and Abdelfatta, 2020).

However, in this study, the observed strong absorption at ~200 nm, coupled with the absence of the expected red-shift, deviates from the typical GO/rGO spectral profile. Absorption in this lower wavelength region is characteristic of small sp^2 carbon domains exhibiting quantum confinement effects. Such behavior aligns more closely with carbon dots or graphene-like nanofragments, where optical properties are governed by the size of conjugated π-domains rather than layered structural interactions. Additionally, the observed peak broadening suggests a distribution of particle sizes or significant structural heterogeneity at the nanoscale (Uddin et al., 2023).

Consequently, the term functionalized carbon nanomaterials (FCNs) is adopted to better describe the material. This classification reflects the presence of nanoscale sp^2 carbon clusters with surface functional groups, without implying the extended layered structure of GO or the restored network of rGO, thereby aligning with observed optical behavior (Ochigbo et al., 2024).

3.1.2 Fourier Transform Infrared (FTIR) Spectroscopy Analysis

The surface chemistry of the synthesized biomass-derived nanocarbon was investigated using FTIR spectroscopy (Figure 3). The analysis confirmed the presence of abundant oxygen-containing functional groups on the carbon surface. Characteristic broad absorption bands observed in the region of approximately 3200–3600 cm^{-1} correspond to the O–H stretching vibration of hydroxyl groups, including those from phenol, alcohol, or carboxyl functionalities, as well as adsorbed water molecules. Furthermore, distinct peaks in the range of 1700–1720 cm^{-1} are attributable to the C=O stretching vibration of carbonyl and carboxyl (–COOH) groups. Additional bands around 1000–1300 cm^{-1} are indicative of C–O stretching vibrations present in ethers, alcohols, and carboxylic acids.

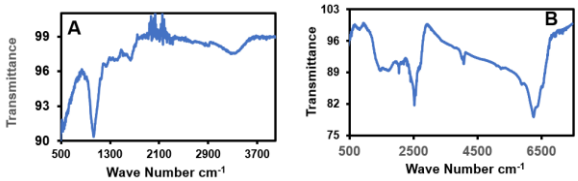

Figure 3: FTIR Analysis Results Comparing Free Goose Grass as Control (A) and Goose Grass Synthesised Graphene (B)

The presence of these oxygen-rich surface functionalities is critically important for the materials application potential, particularly in environmental remediation and catalysis. These groups, especially –OH and –COOH, serve as active sites that can significantly enhance the materials hydrophilicity, facilitating better dispersion in aqueous media. More importantly, they are well-documented to play a pivotal role in the adsorption of various species. They act as binding sites for metal ions through

mechanisms such as surface complexation and ion exchange, where protons from carboxyl groups can be displaced by metal cations (M^{2+}) from solution. This functional group-rich surface is a key characteristic of carbon materials derived from biomass precursors, which often retain a degree of their original organic structure after carbonization. (Li et al., 2024).

3.1.3 X-ray Diffraction (XRD) Analysis

The structural order and phase composition of the carbon material were examined using X-ray diffraction (XRD) and presented in figure 4. The diffraction pattern exhibited broad, diffuse peaks, which are characteristic of amorphous or highly disordered carbon structures. A prominent, broad reflection was observed in the 2θ range of approximately 22–24°, corresponding to the (002) plane of graphitic carbon. The broad nature of this peak indicates a lack of long-range order along the stacking direction of the graphene layers. This specific feature is typical of a *turbostratic* carbon structure, where the graphitic layers are roughly parallel to each other but exhibit random rotation or translation, resulting in a disordered stacking arrangement and a larger interlayer spacing compared to the highly ordered structure of crystalline graphite (Taj et al.,2024).

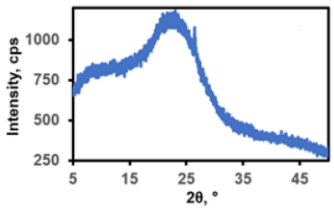

Figure 4: XRD Analysis Results for Goose Grass Synthesised Graphene

In contrast to the sharp (002) peak of well-graphitized carbon, which appears near 26°, the shift to a. lower angle (22–24°) for this material further confirms an increased interlayer spacing (d_{002}), a hallmark of turbostratic disorder. The absence of sharp, high-intensity peaks also rules out the presence of a highly crystalline graphene phase. This defect-rich, turbostratic structure is commonly observed in carbons produced through low-temperature carbonization of organic precursors like biomass, where the thermal energy is insufficient to drive complete graphitization. Such a structure often contributes to a high density of edge-plane defects, which can serve as additional active sites.

3.1.4 Scanning Electron Microscopy (SEM) Analysis

The morphological features of the as-synthesized nanocarbon were visualized using Scanning Electron Microscopy (SEM). The micrographs (Figure 5) revealed a surface morphology consisting of highly crumpled, folded, and aggregated nanosheets, interspersed with irregularly shaped particles. This morphology is a direct consequence of the top-down breakdown of the larger biomass cellular structure during the carbonization and subsequent processing steps. The crumpled sheet-like texture is reminiscent of exfoliated or reduced graphene oxide but with a higher degree of disorder and aggregation, which is consistent with the turbostratic structure identified by XRD.

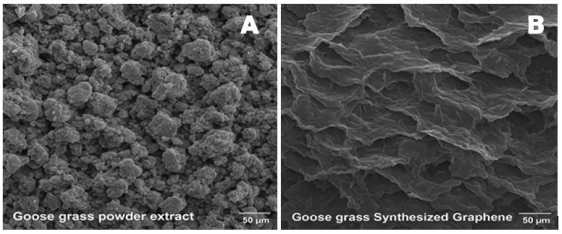

Figure 5: SEM Micrographs of at 50 µm magnification for *Goose Grass Powder* extract (control) and *Goose Grass* synthesized Graphene.

The observed aggregation is a common phenomenon for nanomaterials, driven by van der Waals forces between the thin carbon layers, which act to minimize the high surface energy of the individual nanosheets. The combination of nanosheets and nanoparticles creates a complex, multi-dimensional architecture. This interconnected, aggregated network is beneficial for applications such as adsorption and energy storage, as it can generate a hierarchical pore structure. Micropores and mesopores may exist within the crumpled sheets and between aggregated particles, contributing to a high specific surface area and providing pathways for the rapid transport of ions or molecules to the active sites located on the surfaces of the nanosheets (Shaw et al.,2024).

3.2 Agronomic Performance

3.2.1 Effects of Goose Grass–Derived Carbon Nanomaterials on Plant Growth

This section presents and discusses the effects of functionalized carbon nanomaterials (FCNs) derived solely from goose grass (*Eleusine indica*) on plant growth, in comparison with control, organic manure, and synthetic fertilizer treatments. The primary objective was to evaluate the influence of these treatments on key growth parameters plant height, number of leaves, and leaf width over a five-week growth period (Agegnehu et al.,2024). The results are interpreted alongside existing literature on carbon-based nanofertilizers to elucidate their roles in nutrient delivery, growth regulation, and vegetative development. Field results demonstrate that FCN-treated plots exhibited delayed but sustained vegetative growth, consistent with adsorption-mediated nutrient release. By week five,

growth parameters approached those of synthetic fertilizer treatments, though early-stage performance remained inferior. These findings support the role of FCNs as nutrient-delivery enhancers, not standalone fertilizers (Das et al.2023).

3.2.1.1 Week One (Establishment Phase)

Du8ring the first week of growth, plants treated with organic manure attained the greatest mean height (1.8 cm), while those treated with goose grass–derived FCNs exhibited a modest improvement over the control (Table 1). The FCN treatment resulted in a mean height of 1.1 cm compared with 0.7 cm in the control. Leaf number remained low (2–3 leaves), and differences in leaf width were minimal across treatments.

Table 1: Plant growth parameters in week one

Treatment	Height (cm)	Number of leaves	Leaf width (cm)
Control	0.7	2	1.4
Organic manure	1.8	2	1.4
Synthetic fertilizer	1.0	3	1.3
Nanofertilizer (Goose grass)	1.1	3	1.2

The limited early response observed under the FCN treatment is consistent with the slow-release behavior of carbon-based nutrient systems. Owing to their high surface area and nutrient-binding capacity, functionalized carbon nanomaterials often delay nutrient availability during early establishment stages, as nutrients are adsorbed onto the material's surface rather than being immediately accessible to plant roots (Das et al., 2023).

3.2.1.2 Week Two (Emergent Nutrient Uptake Phase)

By the second week, a marked increase in plant height was recorded across all treatments (Table 2). Synthetic fertilizer produced the tallest plants (4.1 cm), followed by the goose grass FCNs (3.5 cm). Plants under the FCN treatment developed four leaves, exceeding the control and equaling organic manure.

Table 2: Plant growth parameters in week two

Treatment	Height (cm)	Number of leaves	Leaf width (cm)
Control	2.0	3	1.5
Organic manure	2.2	4	1.5
Synthetic fertilizer	4.1	3	1.7
Nanofertilizer (Goose grass)	3.5	4	1.6

The improved performance of the goose grass FCNs at this stage suggests enhanced nutrient uptake resulting from gradual nutrient release (de Barros et al.2023 and Mirza et al. 2022). The oxygen-containing functional groups on the carbon nanomaterial surface facilitate the adsorption of nutrient ions, which are subsequently released into the soil solution as plant demand increases (Mukarram et al., 2022). Similar improvements in nutrient-use efficiency have been reported for crops treated with graphene oxide-based nanomaterials (Zhang et al., 2022).

3.2.1.3 Week Three (Active Vegetative Stage)

At week three, treatment effects became more pronounced (Table 3). Plants receiving synthetic fertilizer attained the greatest height (7.4 cm), followed by the goose grass FCNs (5.0 cm), both outperforming organic manure and control treatments. Leaf width under the FCN treatment (1.9 cm) was substantially greater than that of the control.

Table 3: Plant growth parameters in week three

Treatment	Height (cm)	Number of leaves	Leaf width (cm)
Control	2.5	3	1.6
Organic manure	3.0	4	1.7
Synthetic fertilizer	7.4	5	2.4
Nanofertilizer (Goose grass)	5.0	4	1.9

The improved vegetative growth observed under the goose grass FCNs may be attributed to the presence of oxygen-containing functional groups on the carbon surface, which enhance nutrient adsorption and sustained release (Perumal et al. 2022). These functional groups can interact with cationic nutrients such as ammonium (NH_4^+) and potassium (K^+), creating a reservoir that supplies nutrients in sync with plant growth requirements (Bansal et al., 2025).

3.2.1.4 Week Four (Maturity Onset)

In the fourth week, growth acceleration was evident across treatments (Table 4). The goose grass FCNs (8.5 cm) significantly outperformed organic manure (5.5 cm) and control (3.7 cm), though synthetic fertilizer maintained the highest mean height (10.5 cm).

Table 4: Plant growth parameters in week four

Treatment	Height (cm)	Number of leaves	Leaf width (cm)
Control	3.7	4	1.9
Organic manure	5.5	4	2.0
Synthetic fertilizer	10.5	5	3.5
Nanofertilizer (Goose grass)	8.5	4	2.7

The sustained growth under the goose grass FCNs supports its role as a controlled-release nutrient system. Comparable trends have been reported in studies where graphene-based nanocomposites prolonged nutrient availability relative to conventional fertilizers. For instance, de Barros et al. (2023) demonstrated that urea-functionalized graphene oxide provided prolonged nitrogen release, supporting crop growth over extended periods compared to conventional urea (Qiao et al. 2024).

3.2.1.5 Week Five (Peak Productivity Phase)

By week five, plants treated with synthetic fertilizer achieved the highest overall growth. However, the goose grass FCNs closely approached this performance, achieving a mean height of 11.0 cm, five leaves, and a leaf width of 4.0 cm (Table 5).

Table 5: Plant growth parameters in week five

Treatment	Height (cm)	Number of leaves	Leaf width (cm)
Control	4.3	4	2.1
Organic manure	8.7	5	3.0
Synthetic fertilizer	13.0	6	5.0
Nanofertilizer (Goose grass)	11.0	5	4.0

The consistent growth observed under the goose grass FCNs from week two onward demonstrates its effectiveness as a sustainable alternative or complement to synthetic fertilizers, providing prolonged nutrient availability and enhanced vegetative development. (Singh et al. 2024 and Wang et al. 2023) The convergence of growth parameters between FCN and synthetic fertilizer treatments by week five confirms the role of carbon nanomaterials as nutrient-delivery enhancers that can reduce reliance on conventional fertilizers while maintaining crop productivity. These findings align with the valorization of *Eleusine indica* biomass into value-added agricultural inputs, supporting circular economy principles in sustainable agriculture (Zhang et al. 2022).

3.2.1.6 Statistical Analysis and Interpretation of Plant Growth Parameters

A one-way Analysis of Variance (ANOVA) was used to evaluate the effects of four treatments—control, organic manure, synthetic fertilizer, and *Eleusine indica* (goose grass)-derived graphene nanofertilizer—on plant growth over five weeks. Mean separation employed Fisher's Least Significant Difference (LSD) at $p \leq 0.05$, though full ANOVA tables and repeated-measures analysis are needed for confirmatory inference (Gomez and Gomez 2021).

No significant differences were observed in week one ($p > 0.05$), indicating similar initial growth. However, significant differences emerged from week two, becoming highly significant by weeks four and five ($p < 0.001$), suggesting a cumulative treatment effect consistent with controlled-release behavior (Rezvani and Bahrami 2022).

The graphene nanofertilizer consistently outperformed the control and organic manure treatments. By week five, its performance in plant height and leaf width was statistically comparable to synthetic fertilizer, while remaining superior to the other treatments.

This enhanced performance is attributed to controlled nutrient release, improved nutrient uptake, and possible physiological stimulation at the plant–nanomaterial interface. The sustained growth aligns with expected slow-release properties of carbon-based nanofertilizers. These findings support earlier studies showing improved biomass and reduced nutrient losses (Singh et al., 2024; Anand et al., 2022), and confirm that biomass-derived carbon nanomaterials can rival conventional fertilizers (Kumar and Singh, 2023).

Overall, the nanofertilizer demonstrated strong potential as an eco-friendly alternative. Future studies should include field trials, soil–microbe interactions, nutrient-use efficiency, and comprehensive statistical analyses.

3.2.1.7 AAS Results Analysis

Atomic Absorption Spectrophotometry (AAS) was employed to quantify the uptake of essential macro- and micronutrients (Ca, Fe, K, Mg, and Zn) in plant tissues following fertilizer application. The technique provided reliable elemental detection at element-specific wavelengths, consistent with established analytical protocols for plant nutrient analysis. Variations in corrected absorbance, calibrated concentrations, and sample concentrations across treatments clearly demonstrate the influence of fertilizer type on nutrient availability and plant uptake

efficiency. Furthermore, recent advances in nanotechnology highlight the potential of functionalized carbon-based nanomaterials to act as carriers for such micronutrients, facilitating their controlled release and translocation within plants (Ashfaq et al.,2025).

The control column sample (Table 6) represents baseline nutrient levels in the absence of fertilizer input. Calcium and potassium exhibited relatively higher concentrations compared to other elements, suggesting their natural abundance in the growth medium. However, magnesium and zinc were present at very low concentrations, indicating potential nutrient limitation under unfertilized conditions.

Table 6: Control Column Sample Analysis

Parameter	Ca	Fe	K	Mg	Zn
Wavelength (nm)	422.67	248.33	404.41	285.21	213.86
Corrected Absorbance	0.3811	0.0709	0.0232	1.5904	0.2779
Concentration (Calib)	16.96	1.281	31.26	2.372	0.722
Standard Deviation	0.80	9.55	0.73	0.06	0.34
Concentration in mg/L (Sample)	0.135	0.1224	0.228	0.0014	0.0024
Standard Deviation in mg/L (Sample)	0.80	9.55	0.73	0.06	0.34
%RSD	0.80	9.55	0.73	0.06	0.34

3.2.1.7.1 Nutrient Status in the Control Sample

The generally low %RSD values (≤9.55%) indicate acceptable analytical precision, aligning with recommended limits for AAS-based elemental analysis. These findings confirm that without fertilizer amendment, nutrient uptake by plants remains minimal and largely dependent on inherent soil reserves. (Skoog, et al.2023).

3.2.1.7.2 Effect of Goose Grass without Fertilizer Application

Goose grass samples (Table 7) showed marginal increases in potassium concentration relative to the control, while iron and zinc levels declined. This trend suggests that goose grass, as a fast-growing weed species, may preferentially uptake available macronutrients such as potassium while competing poorly for micronutrients under nutrient-limited conditions (Zulqarnain et al. 2025).

Table 7: Goose Grass Sample Analysis

Parameter	Ca	Fe	K	Mg	Zn
Wavelength (nm)	422.67	248.33	404.41	285.21	213.86
Corrected Absorbance	0.3889	0.0399	0.0235	1.1047	0.5511
Concentration (Calib)	17.30	0.722	31.70	1.648	1.432
Standard Deviation	0.72	5.07	1.56	0.13	0.03
Concentration (Sample)	0.125 mg/L	0.0366 mg/L	0.496 mg/L	0.0021 mg/L	0.0004 mg/L
Standard Deviation (Sample)	0.72 mg/L	5.07 mg/L	1.56 mg/L	0.13 mg/L	0.03 mg/L
%RSD	0.72	5.07	1.56	0.13	0.03

Similar nutrient partitioning behaviour has been reported in grasses with high metabolic demand for potassium to support osmotic regulation and photosynthesis. The low iron concentration may also reflect reduced bioavailability in the absence of chelating agents or fertilizer-derived iron sources.

3.2.1.7.3 Influence of Organic Manure on Nutrient Uptake

Organic manure treatment (Table 8) resulted in notably higher calibrated concentrations of calcium, iron, and magnesium, indicating improved nutrient availability following organic amendment. Although the measured sample concentrations remained relatively low, the enhanced absorbance signals suggest gradual nutrient mineralization from organic matter. Studies have shown that organic fertilizers can produce effects on plant growth and nutrient uptake comparable to synthetic fertilizers, primarily through the slow release of nutrients. Furthermore, the positive effect on iron uptake aligns with findings that carbon-based nanomaterials, which can be present in amended soils, may assist in micronutrient delivery to plants (Bankar et al. 2021).

Table 8: Organic Manure Sample Analysis

Parameter	Ca	Fe	K	Mg	Zn
Wavelength (nm)	422.67	248.33	404.41	285.21	213.86
Corrected Absorbance	0.5649	1.1002	0.0239	1.4915	0.0649
Concentration (Calib)	25.13	19.89	32.24	2.225	0.169
Standard Deviation	0.06	0.08	0.68	0.11	0.83
Concentration (Sample)	0.015 mg/L	0.015 mg/L	0.219 mg/L	0.0024 mg/L	0.0014 mg/L
Standard Deviation (Sample)	0.06 mg/L	0.08 mg/L	0.68 mg/L	0.11 mg/L	0.83 mg/L
%RSD	0.06	0.08	0.68	0.11	0.83

Organic fertilizers are known to improve soil structure and microbial activity, thereby enhancing micronutrient solubility and root uptake over time. The elevated iron response in particular highlights the role of organic ligands in maintaining iron in plant-available forms, reducing fixation in soil matrices (Sharma and Kumar 2025).

3.2.1.7.4 Impact of Synthetic Fertilizer Application

The synthetic fertilizer-treated goose grass sample (Table 9) exhibited the highest potassium concentration among all treatments, alongside increased calcium and iron uptake compared to the control. This reflects the rapid nutrient release characteristic of inorganic fertilizers, which provide readily soluble ions for immediate plant absorption (Sharma and Kumar 2025).

Table 9: Synthetic Goose Grass Sample Analysis

Parameter	Ca	Fe	K	Mg	Zn
Wavelength (nm)	422.67	248.33	404.41	285.21	213.86
Corrected Absorbance	0.4155	1.0744	0.0242	1.4452	0.0888
Concentration (Calib)	18.49	19.43	32.59	2.156	0.231
Standard Deviation	0.36	0.19	1.34	0.03	0.52
Concentration (Sample)	0.066 mg/L	0.036 mg/L	0.436 mg/L	0.0007 mg/L	0.0012 mg/L
Standard Deviation (Sample)	0.36 mg/L	0.19 mg/L	1.34 mg/L	0.03 mg/L	0.52 mg/L
%RSD	0.36	0.19	1.34	0.03	0.52

However, magnesium and zinc concentrations remained comparatively low, suggesting possible nutrient antagonism or dilution effects caused by high potassium availability. Such interactions are well-documented, where excessive K^+ can suppress Mg^{2+} and Zn^{2+} uptake at the root interface

3.2.1.8 Methodological Considerations and Data Quality

While the elemental uptake data suggest improved nutrient availability under fertilized treatments, internal inconsistencies in the reported standard deviations and the uniformly low absolute concentrations in the samples warrant caution. The large standard deviations for some elements (e.g., Fe in control samples) relative to their mean values indicate potential issues with sample heterogeneity or analytical precision. Furthermore, the low sample concentrations several orders of magnitude below the calibrated concentrations suggest that the sample digestion, dilution factors, and calibration protocols require refinement before quantitative conclusions can be drawn (Pandey et al. 2024). For instance, the use of secondary wavelengths or alternative sample preparation procedures could help accommodate the wide concentration ranges between macro- and micronutrients in plant tissues (Lamouchi et al.2025). Therefore, while the trends observed between treatments are informative, the absolute values should be interpreted as semi-quantitative at this stage.

4. Conclusion

This study demonstrates the successful valorisation of *Eleusine indica* biomass into functionalized carbon nanomaterials and establishes their applicability as nutrient-delivery carriers in agricultural systems. Comprehensive physicochemical characterization confirms that the synthesized material is more accurately classified as oxygen-functionalized carbon nanodots or graphene-like nanocarbon rather than pristine graphene, as evidenced by UV–Vis absorption behavior, FTIR functional group analysis, XRD turbostratic structure, and SEM morphology. These features collectively endow the material with high surface reactivity and adsorption capacity, which are essential for controlled nutrient interactions.

Field evaluation revealed that the functionalized carbon nanomaterial–based formulation exhibited a delayed yet sustained agronomic response, consistent with adsorption-mediated nutrient release mechanisms. While early growth performance was inferior to that of conventional synthetic fertilizer, vegetative growth parameters under the nanomaterial treatment converged with synthetic fertilizer by the later growth stages. Statistical analysis confirmed that from week two onward, treatment effects were significant, and by week five, no significant differences were observed between nanomaterial and synthetic fertilizer treatments for key growth indicators. These findings reinforce the role of biomass-derived carbon nanomaterials as nutrient-use efficiency enhancers rather than direct nutrient sources.

In summary, the results highlight the dual environmental and agronomic value of converting an invasive weed into a functional agricultural input, aligning with circular bioeconomy and sustainable intensification principles. Nevertheless, further work is required to strengthen material classification and mechanistic understanding through advanced techniques such as Raman spectroscopy, XPS, and TEM, alongside nutrient-release kinetics, long-term yield studies, and comprehensive soil–plant–microbe interaction assessments. With such validation, *Eleusine indica*–derived functional carbon nanomaterials hold strong potential as scalable, eco-friendly components of next-generation fertilizer systems.

Conflict of Interest

The authors declare no conflict of interest.

References

1. Agegnehu, G., Nelson, P. N., and Bird, M. I. (2024). The role of organic amendments in improving soil fertility and crop productivity: A global meta-analysis. *Agriculture, Ecosystems and Environment, 352*, 108460. https://doi.org/10.1016/j.agee.2023.108460
2. Anand, K. V., Aanand, S., and Kumar, M. (2022). Graphene-based nanomaterials for sustainable agriculture: Synthesis, mechanisms, and applications. *Journal of Nanobiotechnology*, 20(1), 1-22. https://doi.org/10.1186/s12951-022-01345-7
3. Ashfaq, M., Gupta, G., and Verma, N. (2025). Carbon-based nanocarriers for plant growth promotion: Fuelling when needed. Nanoscale, 17(2), 616–634. https://doi.org/10.1039/D4NR03268C
4. Bankar, A., Kamble, M., Dhenge, S., Bhoyar, T., and Mungole, A. (2021). Carbon nanodots derived from kitchen waste biomass as a growth accelerator for fenugreek plant. Journal of Nanoscience and Nanotechnology, 21(4), 2432–2440. https://doi.org/10.1166/jnn.2021.18976
5. Bansal, K., Rana, N., and Singh, P. (2025). Surface-functionalized carbon nanomaterials for controlled agrochemical release: A review. *Journal of Environmental Management*, 375,

124321. https://doi.org/10.1016/j.jenvman.2025.124321

6. Chen, H., Yada, R., and Li, J. (2022). Carbon-based nanomaterials for sustainable agriculture: Nutrient delivery and soil interaction mechanisms. *Environmental Science: Nano, 9*(5), 1542–1560. https://doi.org/10.1039/D2EN00047A
7. Chen, X., Feng, Y., and Zhou, W. (2022). Sustainable approaches for biomass-derived carbon nanomaterials. Renewable and Sustainable Energy Reviews, 154, Article 111861. https://doi.org/10.1016/j.rser.2021.111861
8. Das, S., Sen, S., and Mandal, D. (2023). Carbon nanomaterials as smart nutrient carriers in agriculture. *Journal of Cleaner Production, 382*, 135311. https://doi.org/10.1016/j.jclepro.2022.135311
9. de Barros, C. H. N., de Souza, A. P. C., and Seabra, A. B. (2023). Functionalized graphene oxide for sustained nutrient delivery in agricultural systems. *Journal of Cleaner Production*, 385, 135712. https://doi.org/10.1016/j.jclepro.2022.135712
10. Gamal, A., Tang, M., Chehimi, M. M., El-Hussieny, H., and Ahmed, M. (2025). Effect of metal loading and Ce addition on biochar-supported Co catalysts for CO2 methanation. Biochar, 7, 73. https://doi.org/10.1007/s42773-025-00428-0
11. Gomaa, M. and Abdel Fattah, G. (2020) 'Optical properties of graphene oxide thin film reduced by low-cost diode laser', *Applied Physics A*,126, 519. https://doi.org/10.1007/s00339-020-03710-3 .
12. Gomez, K. A., and Gomez, A. A. (2021). *Statistical Procedures for Agricultural Research* (3rd Ed.). Wiley-Blackwell.
13. Kumar, R., and Singh, S. (2023). Carbon-based nanofertilizers for controlled nutrient release in crop production: A review. *Environmental Science: Nano*, 10(4), 987-1005. https://doi.org/10.1039/D2EN00987A
14. Lamouchi, H., Pistocchi, C., Marsden, C., Ait-Mouheb, N., and Leauthaud, C. (2025). Homemade dry manure tea is equivalent to synthetic fertilizer for the growth and nutrition of spinach. Journal of Soil Science and Plant Nutrition. Advance online publication. https://doi.org/10.1007/s42729-024-02144-3
15. Li, Q., Li, F., XXX, Y., Yu, C., Yan, H., Zheng, M., and Chen, H. (2024). Research progress in regulation of nanostructure of carbon materials and adsorption of toxic pollutants in water. *Cailiao Gongcheng/Journal of Materials Engineering*, 52(10), 57–69. https://doi.org/10.11868/j.issn.1001-4381.2023.000695
16. Mirza, H., Khan, M., and Shahid, M. (2022). Interaction of graphene-based nanomaterials with soil–plant systems. *Science of the Total Environment, 807*, 150850. https://doi.org/10.1016/j.scitotenv.2021.150850
17. Mukarram, M., Choudhary, S., Kurjak, D., Petek, A., and Khan, M. M. (2022). Graphene-based nanomaterials in agricultural systems: A systematic review of applications and mechanisms. *Chemosphere*, 308, 136365. https://doi.org/10.1016/j.chemosphere.2022.136365
18. Nguyen, V. H., and Nguyen, T. A. (2024). Raman and XPS insights into carbon nanomaterial functionalization strategies. Analytical Methods, 16(1), 55–73. https://doi.org/10.1039/D3AY01956A
19. Ochigbo, S. S., Obar, A. O., Suleiman, M., and Kovo, A. (2024). Facile synthesis and optimization of graphene oxide reduction by annealing in hydrazine vapour in ambient air for potential application in perovskite solar cells. *Science World Journal*, *19*(1), 194-199. https://doi.org/10.4314/swj.v19i1.26
20. Pandey, K., Omar, R. A., Verma, N., and Gupta, G. (2024). Fe–carbon nanofiber-modified Mo-MOF for the controlled release and translocation of micronutrients in plants. Environmental Science: Nano, 11(4), 1597–1611. https://doi.org/10.1039/D3EN00866A
21. Perumal, S., Sankaranarayanan, R., and Subramanian, V. (2022). Green and chemical synthesis of graphene derivatives: A comparative review. *Journal of Materials Chemistry A, 10*(32), 16648–16672. https://doi.org/10.1039/D2TA02891A
22. Qiao, Y., Zhang, X., Li, Q., and Zhou, D. (2024). Physiological responses of crops to graphene-based soil amendments. *Environmental Nanotechnology, Monitoring and Management, 22*, 100754. https://doi.org/10.1016/j.enmm.2024.100754
23. Rezvani, M., and Bahrami, H. (2022). Field experimental design and analysis: A practical review. *Frontiers in Agronomy*, **4**, 893212. DOI: 10.3389/fagro.2022.893212
24. Sharma, A., and Kumar, V. (2025). Comparative evaluation of organic and synthetic fertilizers on lettuce yield and metabolomic profiles. Horticulturae, 11(12), 421. https://doi.org/10.3390/horticulturae11121421
25. Shaw, V., Koley, R., Das, S., Saha, T., and Mondal, N. K. (2024). Sustainable use of plastic-derived nanocarbons as a promising

larvicidal and growth inhibitor agent towards control of mosquitoes. *Science of The Total Environment*, 921, 171055. https://doi.org/10.1016/j.scitotenv.2024.171055

26. Singh, A., Sharma, R., and Gupta, V. (2024). Biomass-derived graphene quantum dots as efficient nanofertilizers for enhanced crop productivity and reduced environmental impact. *ACS Sustainable Chemistry and Engineering*, 12(2), 845-860. https://doi.org/10.1021/acssuschemeng.3c05678
27. Singh, A., Verma, S., and Singh, N. B. (2024). Nanofertilizers: Mechanisms, agronomic efficiency, and environmental safety. *Critical Reviews in Environmental Science and Technology, 54*(6), 721–758. https://doi.org/10.1080/10643389.2023.2178921
28. Skoog, D. A., West, D. M., Holler, F. J., and Crouch, S. R. (2023). Fundamentals of analytical chemistry (10th ed.). Cengage Learning.
29. Taj, M., Bhat, V. S., Sriram, G., Kurkuri, M., Manohara, S. R., De Padova, P., and Hegde, G. (2024). PEDOT-doped mesoporous nanocarbon electrodes for high capacitive aqueous symmetric supercapacitors. *Nanomaterials*, 14(14), 1222. https://doi.org/10.3390/nano14141222
30. Tiba, D. Y., and Canevari, T. C. (2025). Graphene hybrid nanostructures based screen-printed sensor employed in the glyphosate electrocatalytic determination in the real sample. Materials Research Bulletin, 185, 113290. https://doi.org/10.1016/j.materresbull.2024.113290
31. Uddin, J., Roy, A.K. and Ghann, W.E. (2023) '(Digital Presentation) Hydrogen Peroxide Assisted Fluorescent Carbon Nanoparticles from Teak Leaves', *Meet. Abstr.*, MA2023-01, 2834. https://doi.org/10.1149/MA2023-01172834mtgabs .
32. Wang, Y., Liu, R., and Zhao, Y. (2023). Graphene-derived carbon nanomaterials in agroecosystems: Fate, transport, and plant response. *Journal of Hazardous Materials, 442*, 130047. https://doi.org/10.1016/j.jhazmat.2022.130047
33. Yahaya, M. I., and Salihu, Z. (2024). Efficiency of green synthesised carbon nanotubes from Moringa oleifera leaf extract as potential toxic metals adsorbent in polluted water. Pure and Applied Chemistry. Advance online publication. https://doi.org/10.1515/pac-2024-0103
34. Zamora-Ledezma, E., Zamora-Ledezma, C., and Clavijo, M. (2025). Phytotoxic effects and agricultural potential of nanofertilizers: A study using zeolite, zinc oxide, and titanium dioxide under controlled conditions. Journal of Xenobiotics, 15(4),123. https://doi.org/10.3390/jox15040123
35. Zhang, X., Chen, G., and Li, Y. (2022). Graphene and graphene oxide in plant systems: Interactions, mechanisms, and applications. *Environmental Science: Nano, 9*(3), 828–856. https://doi.org/10.1039/D1EN01091H
36. Zulqarnain, H., Akbar, M., Ahmad, A., Farooq, U., Alshaya, H., and Ali, H. M. (2025). Engineered carbon dots as plant nanobionics: Mechanistic insights of biodegradation, nutrient delivery, and gene modulations for smart sustainable agriculture. Critical Reviews in Plant Sciences, 44(3), 139–179. https://doi.org/10.1080/07352689.2025.2529740

